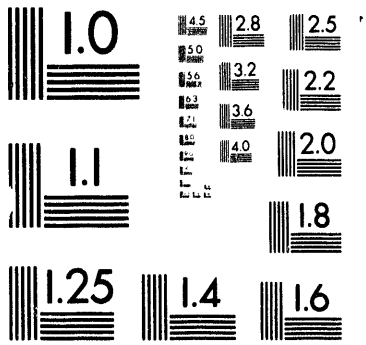
1.0
1.1
1.25
1.4
1.6
1.8
2.0
2.2
2.5
2.8
3.2
3.6
4.0
4.5
5.0
5.6
6.3
7.1
8.0
9.0

1 of 1

Conf-940326--5
SAND93-2334C

ISOTHERMAL CORROSION TESTING OF STEELS IN MOLTEN NITRATE SALTS *

Michael R. Prairie, Sammy R. Dunkin, James M. Chavez
Advanced Energy Technology Center
Sandia National Laboratories
Albuquerque, New Mexico

Robert W. Bradshaw, Steven H. Goods
Center for Materials and Applied Mechanics
Sandia National Laboratories
Livermore, California

ABSTRACT

Tests were performed to evaluate the corrosivity of several nitrate salt mixtures on the containment materials likely to be used in a molten-salt solar central receiver power plant. The objective of this work was to determine if common salt impurities (e.g., chloride) aggravate corrosion. The test was conducted for 7008 hours on A36 carbon steel at 320 °C and 304 and 316 stainless steels at 570°C. Seven salt mixtures containing a variety of impurity concentrations were used. Corrosion rates were determined by descaled weight loss for coupons that were removed periodically from the melts. The nitrate mixtures were analyzed for changes in impurity levels and the accumulation of soluble corrosion products. The test results indicate generally that corrosion is slow and that impurities do not contribute dramatically to corrosion rates of carbon and stainless steels.

INTRODUCTION

This paper describes a test examining the corrosion of the containment materials likely to be used in a molten-salt solar central receiver (MSSCR) power plant. The heat-transfer fluid in an MSSCR is a mixture of nitrate salts consisting of 60 wt% $NaNO_3$ and 40 wt% KNO_3. The melting point of this mixture is about 220 °C. In an MSSCR, "cold" molten salt near 285 °C is pumped up to a solar receiver where it is heated to about 565 °C. The "hot" salt then flows to a storage tank where it is used to produce steam when necessary. The cold side of the solar power plant will consist of A36 carbon steel operated at a maximum of about 320 °C. The solar receiver will likely be constructed of 316 stainless steel and the rest of the hot loop of 304 stainless steel. The hot-side systems will be operated at about 565 °C.

The work reported here is in support of the 10 MW Solar Two demonstration plant scheduled to go into operation in 1995. In particular, we want to identify the effects of salt impurities on corrosion and help establish design specifications on corrosion allowances for containment and receiver wall thicknesses. Salt impurity levels are important because lower-grade salt containing more impurities costs less than high-grade salt, and large inventories of salt are needed for thermal storage. For example, the Solar Two project will require 1.5×10^6 Kg of salt and a 100 MW plant designed for a 40% capacity factor will require 16.4×10^6 Kg. Currently, solar salts cost between $0.33 and $0.66 per Kg, delivered, depending on grade and supplier.

It is important, therefore, to select the most economical grades of salt that satisfy engineering requirements and do not contain impurities that aggravate corrosion. For example, dissolved chloride may be a concern since it is often found to accelerate corrosion in high-temperature environments [1]. Impurities typically present in commercial nitrate salts include chlorides, perchlorates, sulfates, and carbonates.

While previous studies have established that high-purity nitrates constitute a relatively benign corrosion environment [2], there is little specific information regarding the effects of impurities on corrosion resistance. For chlorides, however, a few papers describe the results of short-duration tests of carbon steel, although at temperatures much higher than our application. The results generally indicate that chloride ion concentrations above 0.3 wt% increase corrosion rates of iron and carbon steels compared to chloride-free melts [3-5]. Therefore, in addition to studying corrosion in mixtures of commercially available nitrate salts, we conducted two tests with elevated chloride levels to investigate directly the role of chloride.

*Contract No. will be put on original

Table 1. Impurity Concentrations (wt%) in the Nitrate Salt Mixtures

	Salt Mixture						
Impurity	1	2	3	4	5	6	7
Chloride	0.040	0.574	0.760	0.260	0.462	0.104	0.060
Perchlorate	0.035	0.032	0.045	0.247	0.316	0.140	0.064
Sulfate	<0.002	<0.002	<0.002	0.146	0.182	0.015	0.011
Carbonate	0.010	0.010	0.006	0.009	0.021	0.009	0.010
Nitrite	0.025	0.028	0.027	<0.001	0.007	0.001	<0.001

Table 2. Nominal Elemental Composition (wt.%) of the Steel Coupons

	Element						
Alloy	C	Mn	Si	Cu	Mo	Cr	Ni
A36	0.29	0.85-1.20	0.15-0.30	0.20	-	-	-
304	0.08	2.0	1.0	-	-	18-20	8-10
316	0.08	2.0	1.0	-	2.0-3.0	16-18	10-14

EXPERIMENTAL

Salt Mixtures

Seven salt mixtures were used in the experiment. Each consisted nominally of 60 wt% $NaNO_3$ and 40 wt% KNO_3. Impurity concentrations are shown in Table 1. These salts were obtained from three suppliers, Coastal Chemical Company, Cedar Chemical Company, and Chilean Nitrate Corporation. Mixtures 2 and 3 were obtained by adding sodium chloride to Mixture 1 in order to examine the effects of chloride in the absence of other compositional variations. Mixture 1 is the standard high-purity solar salt produced by Coastal Chemical Company. Mixtures 4-7 reflect variations in impurity levels in salts from the other manufacturers.

Test Coupons

Rectangular coupons measuring approximately 20 mm x 50 mm x 2 mm of A36 carbon steel, 304 stainless steel and 316 stainless steel were cut from sheet stock, cleaned, alcohol rinsed, and weighed prior to immersion in the salt melts. The nominal compositions of the test alloys are shown in Table 2.

Apparatus

Two steel crucibles (15 cm I.D.) were constructed for each of the seven molten salt mixtures. The seven crucibles housing the carbon steel coupons were operated at 320 °C and were constructed of carbon steel. The remaining seven crucibles were constructed of 304 SS for operation at 560 °C with the 304 SS and the 316 SS coupons. Each crucible was equipped with two 1000 W band heaters and was heavily insulated. Air was sparged into each crucible through a stainless steel tube on a weekly basis to maintain the balance between nitrate and nitrite and to simulate the fact that the salt tanks in a solar power plant will be breathable.

Before use, all the crucibles were oxidized for 24 hr at about 530 °C in a pre-existing molten salt sump. After being cooled and rinsed, each crucible was loaded with about 10 Kg of salt and allowed to stabilize at temperature for up to one week before the experiment was started. Figure 1 shows the external appearance of several of the crucibles and Fig. 2 shows the top view looking into one of the crucibles.

Operation

Coupon pairs were removed at 120, 240, 480, 864, 1608, 2952, 4008, and 7008 hours for examination by descaled weight

Figure 1. Lateral view of several of the salt crucibles. The wiring is for the three thermocouples monitoring salt and sidewall temperatures. The valves and associated tubing are for the air sparge system.

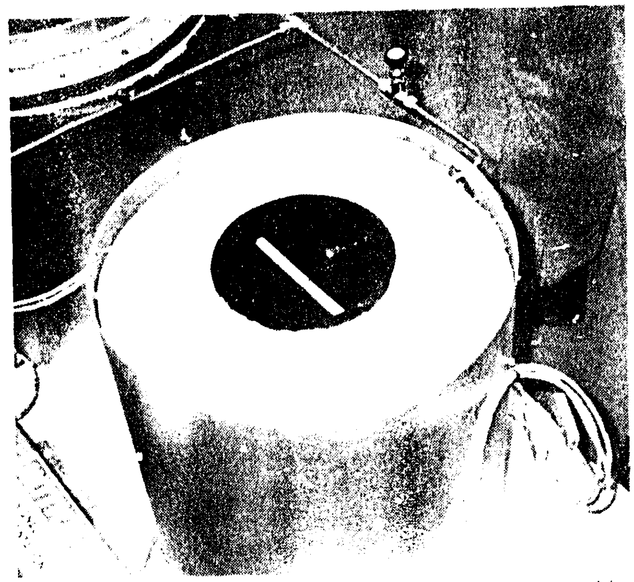

Figure 2. Top view looking down into one of the salt crucibles. The white cross bar is a ceramic rod upon which the coupons are hung in strings of four (strings of one, two for the carbon steel coupons).

loss and metallography. Salt samples were also removed at some of these times and chemically analyzed for impurities and soluble corrosion products.

Analyses

The carbon steel specimens were descaled by immersing them in an inhibited HCl solution at room temperature [6] and the stainless steel specimens were descaled in boiling alkaline permanganate [7]. These solutions removed all corrosion products without significant attack of the underlying metal.

The companion specimens for some of the time intervals were cross-sectioned and prepared for metallographic examination. Optical and scanning electron microscopy, electron microprobe techniques and x-ray diffraction were used to characterize the structure and composition of the adherent corrosion products. Some preliminary metallographic results for this experiment were presented earlier [8] and detailed results from the completed test will be presented elsewhere. The remaining duplicate coupons not used for metallography were descaled to provide additional weight loss information.

The salt samples were analyzed for chloride, nitrite, sulfate, perchlorate, carbonate, pH, alkalinity, chromium, manganese and magnesium by a commercial laboratory.

RESULTS AND DISCUSSION

Weight Loss

Carbon Steel. Weight loss data for the carbon steel coupons are presented in Fig. 3. In general, weight losses were small for all the salt mixtures, corresponding to annualized rates of metal loss ranging between about 1 and 4 μm/yr. The data do not correlate with any measured salt impurity. Even for those specimens immersed in Mixtures 1-3, where the base nitrate salt was identical, increasing chloride concentration did not result in an unambiguous increase in corrosion rate.

These observations are in contrast to previous findings. For example, [illegible] et al. [4] reported that the corrosion rate of mild steel at [illegible] C increased logarithmically with chloride concentration in the range studied. [illegible] et al. [illegible] reported similar results for the corrosion of iron between [illegible] and [illegible] C. The lower temperature employed in our work may contribute to the contrasting behavior.

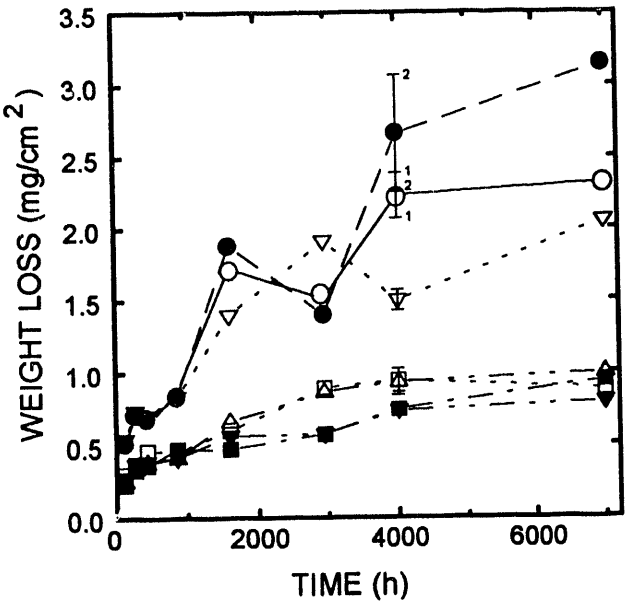

Figure 3. Weight loss data for the corrosion of A36 carbon steel in molten nitrate salt at 320 °C. O-Mixture 1, ●-2, ▽-3, ▼-4, □-5, ■-6, △-7. Error bars show weight loss data for cases where two coupons were available for descaling. Data points are located at the average of the two measurements. Where necessary for clarity, numbers are located adjacent to error marks indicating salt mixture.

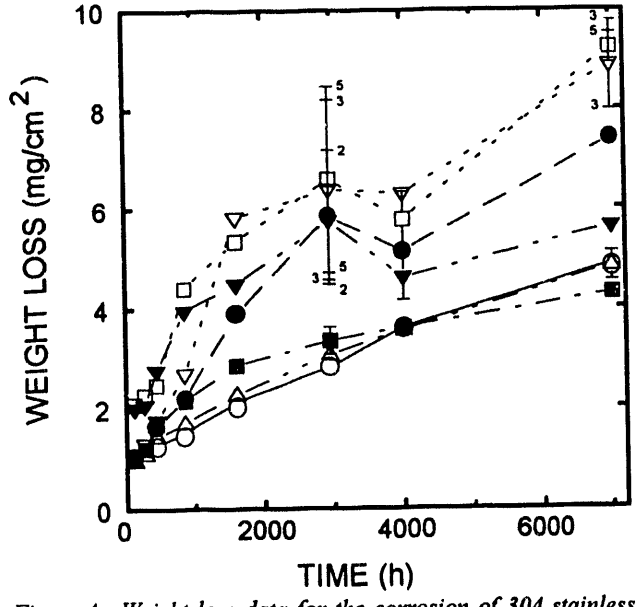

Figure 4. Weight loss data for the corrosion of 304 stainless steel in molten nitrate salt at 570 °C. O-Mixture 1, ●-2, ▽-3, ▼-4, □-5, ■-6, △-7. See Figure 3 for a description of the error bars.

Given the scatter in the data, it is difficult to draw unambiguous conclusions regarding corrosion mechanism. However, weight losses for the mixtures yielding the lowest corrosion rates (4-7) increase monotonically, suggesting adherent, protective oxide layers.

304 Stainless Steel. Figure 4 shows weight loss data for the 304 SS coupons. All of the specimens experienced weight losses of 1-2 mg/cm^2 within the first 100 hr of exposure, followed by much slower corrosion rates.

The results in Fig. 4 generally show that corrosion rate increases with chloride concentration, the effects of which become more pronounced with increasing exposure time. The effect of chloride is particularly evident for the chloride-doped salt Mixtures 2 and 3 in comparison to the high-purity Mixture 1. Corrosion experienced by the 304 SS coupons corresponds to annualized rates of metal loss ranging between about 6 and 12 μm/yr.

For many of the mixtures, especially 4-7, early corrosion appears roughly parabolic, suggesting protective oxide layers. However, as for the carbon steel coupons, the scatter in the data and the absence of a general trend render any determination of a specific corrosion mechanism inconclusive.

316 Stainless Steel. Weight loss data for the 316 SS coupons are shown in Fig. 5. In the salt mixtures containing low levels of chloride (Mixtures 1 and 7), the corrosion rate for 316 SS was about the same as observed for the 304 SS. However, unlike 304 SS, 316 SS appears to be insensitive to chloride in the molten salt environment. Annualized metal loss rates for the 316 coupons in the various salts range between 6 and 9 μm/yr

The 316 SS did not experience the rapid initial corrosion seen after 100 hr for the 304 SS. This difference suggests a surface effect, possibly related to the operations used to fabricate the sheet stock from which the coupons were cut. Indeed, visual inspection of the fresh 304 surface revealed that it was roughly abraded. In contrast, the starting surface of the 316 SS coupons had a smooth, rolled appearance.

As for the 304 SS, a single mechanism for the corrosion of 316 SS is not apparent. Corrosion through non-protective oxides would be first-order in time whereas corrosion through protective layers would exhibit half-order behavior. Our observations generally fall between these two extremes.

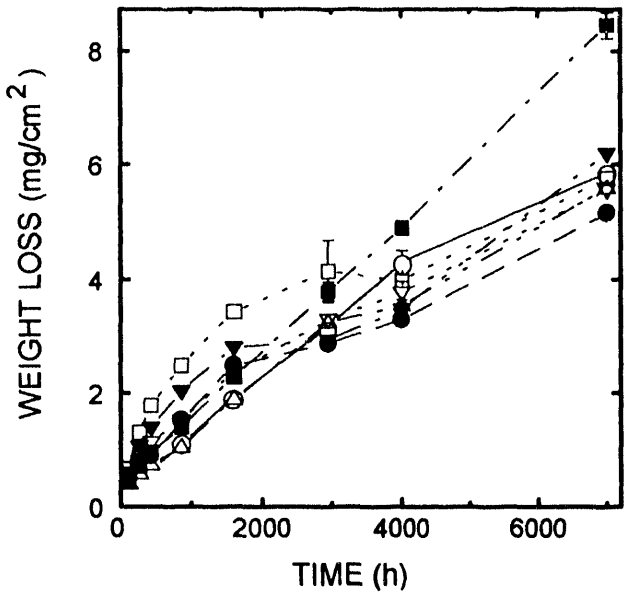

Figure 5. Weight loss data for the corrosion of 316 stainless steel in molten nitrate salt at 570 °C. O-Mixture 1, ●-2, ▽-3, ▼-4, □-5, ■-6, △-7. See Figure 3 for a description of the error bars.

Oxide Spallation

In general, the corrosion layers on the stainless steel alloys demonstrated poor adherence upon cooling to room temperature after long exposure. This is illustrated in Fig. 6 which is a photograph of the stainless steel coupons after exposure for 7008 hr. These coupons were pulled from the hot salt, cooled to room temperature, then rinsed with fresh water. Metallographic characterization of the structure and evolution of the corrosion products was made difficult by the extensive spallation that occurred and the complexity of the oxidation products formed.

Salt Composition

The compositions of the nitrate mixtures were analyzed periodically to monitor the concentrations of the primary impurities and to detect the presence of soluble corrosion products. One of the major changes occurred due to the dissociation of nitrate into nitrite and oxygen. Figure 7 shows the nitrite concentration for the seven mixtures operated at 570 °C. From the initial value of essentially zero for all mixtures, the nitrite concentration increased in the range of 3.5 wt% to 5.5 wt% and then reached a plateau. These values agree well with the calculated value of 3.6 wt% based on equilibrium between nitrate, nitrite, and air at 570 °C [9]. The apparent decline in nitrite concentration between 4000 and 7000 hr may be related to complex interactions between other constituents of the melts (e.g., carbonate). As expected at equilibrium, the concentration of nitrite was negligible in the low-temperature crucibles.

The chloride levels in a number of the high-temperature mixtures increased slightly during the first 1608 hr of the test. These increases occurred in concert with corresponding decreases in perchlorate concentration until all of the perchlorate was converted to chloride. After this, chloride concentrations remained constant in all of the mixtures. Perchlorate conversion was much slower in the low-temperature mixtures.

Sulfate concentrations for the various mixtures were stable during the test. It is notable that the two mixtures that had appreciable sulfate levels (Mixtures 4 and 5) yielded stainless steel coupons having surface scales with a distinctive rust red coloration indicative of hematite (Fe_3O_4). The implication is that the activity of oxygen in mixtures containing sulfate is somewhat higher than in other mixtures, although it is unclear how sulfate itself could cause this. No hematite was observed on carbon steel in any of the mixtures at low temperature.

Figure 8 shows the evolution of carbonate alkalinity in the high-temperature crucibles. Alkalinity increased steadily due to the absorption of carbon dioxide from air sparged through the melts [10]; no free hydroxide was detected. Mixture 4 consistently absorbed more carbon dioxide than the other melts. Inspection of the experimental apparatus revealed no likely source for additional carbon dioxide, nor was a cause for increased mass transfer rate apparent. In any case, no trend in the weight-loss data or any other measurement correlated with the higher alkalinity seen for Mixture 4.

Figures 9 and 10 show the build up of the soluble corrosion products chromium and manganese, respectively, in the high-temperature melts. After the initial rapid accumulation of chromium, due in part to corrosion of the crucibles before coupons were added, chromium concentrated built up slowly. After an early lag, manganese began to accumulate in all of the melts. Then it stabilized after about 3000 hr before declining gradually, possibly as a result of interactions with other chemical constituents present in the melts. In general, all changes in the salt composition were consistent with the thermodynamic processes of the binary nitrate system and with the corrosion processes observed.

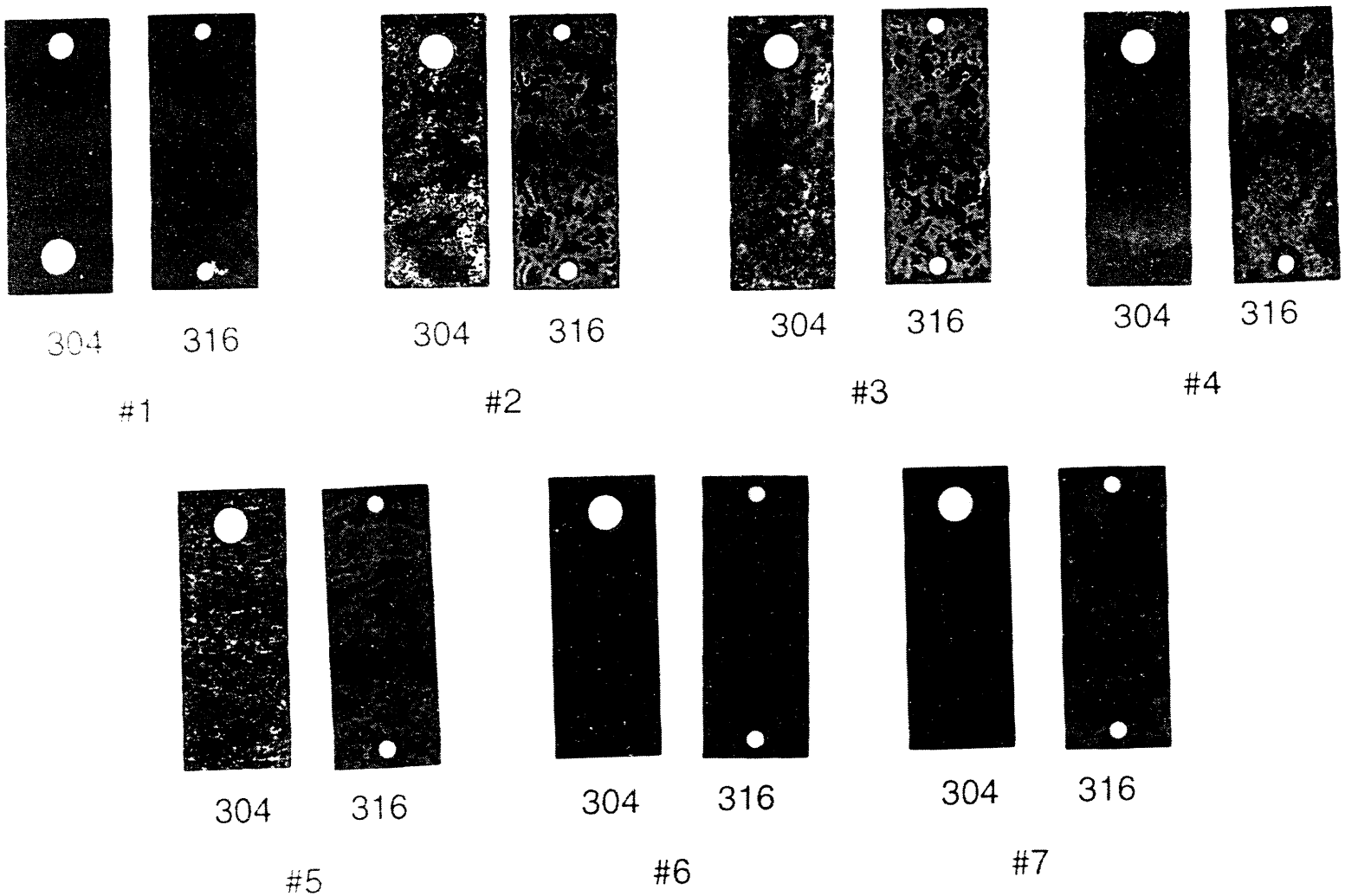

Figure 6. Photograph of the coupons removed from the high-temperature melts after 7008 h

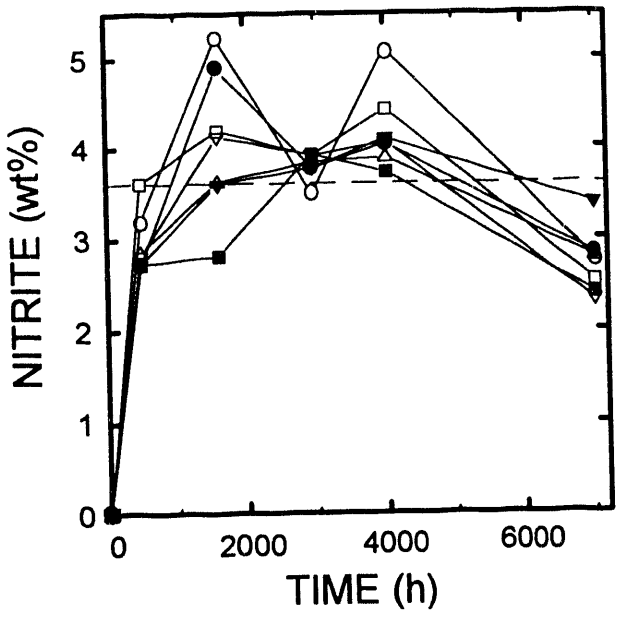

Figure 7. Nitrite in the seven high-temperature mixtures. O-Mixture 1, ●-2, ▽-3, ▼-4, □-5, ■-6, △-7. The dashed line indicates the expected equilibrium concentration based on thermodynamic calculation.

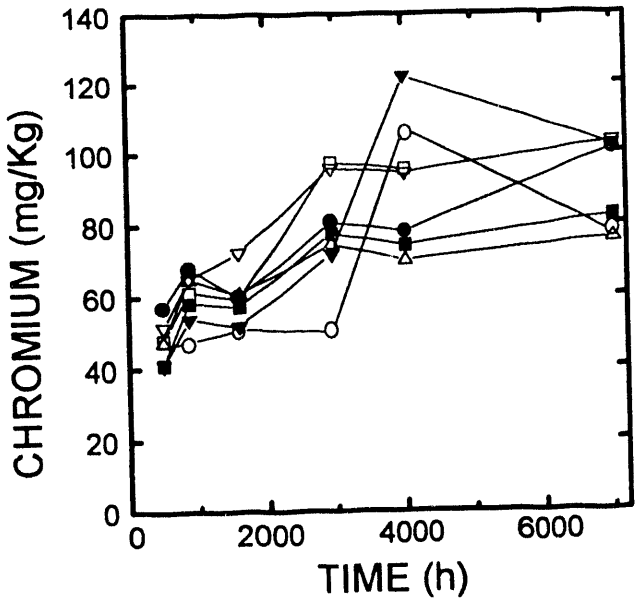

Figure 9. Chromium in the seven high-temperature mixtures. O-Mixture 1, ●-2, ▽-3, ▼-4, □-5, ■-6, △-7.

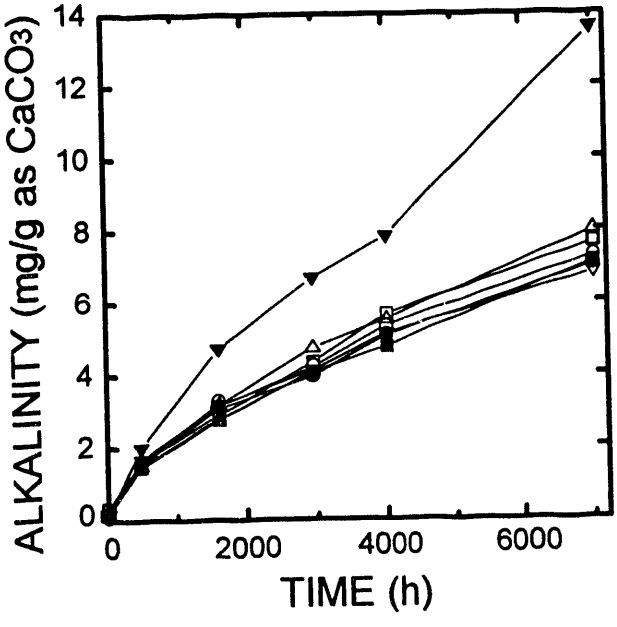

Figure 8. Carbonate alkalinity in the seven high-temperature mixtures. O-Mixture 1, ●-2, ▽-3, ▼-4, □-5, ■-6, △-7.

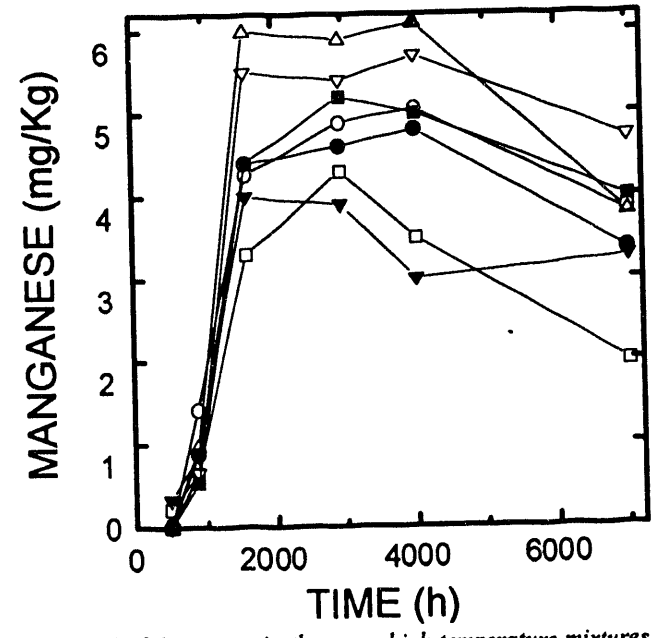

Figure 10. Manganese in the seven high-temperature mixtures. O-Mixture 1, ●-2, ▽-3, ▼-4, □-5, ■-6, △-7.

CONCLUSIONS

This test has demonstrated that molten nitrate salt presents a relatively mild corrosion environment at conditions likely to be employed in a molten-salt solar power plant. At 320 °C, A36 experienced an annualized rate of metal loss ranging between about 1 and 4 μm/yr, and was relatively insensitive to impurities in the salt melt. Corrosion of the 304 and 316 stainless steel alloys at 570 °C was also quite slow, corresponding to annualized metal loss rates ranging between 6 and 12 μm/yr. The corrosion of 304 SS appeared to be slightly sensitive to chloride while no conclusions could be drawn relating the corrosion of 316 SS to any of the measured impurity concentrations. Therefore, salts with impurity levels up to those tested should be acceptable for use in a MSSCR power plant.

The oxide layers on both stainless steel alloys tended to spall when the specimens were cooled to room temperature. This observation may be of critical importance for solar applications of molten nitrate salt technology. Due to the diurnal nature of sunlight and transient cloud cover, the operation of a salt-filled solar receiver is inherently cyclic. Consequently, while directly applicable for the isothermal components of a solar system, we feel that the data described in this report present minimum corrosion rates for the components that would experience transient operation (e.g., the receiver and associated piping). Once spallation occurs, oxide protection afforded by the scale diminishes and corrosion rate increases. Future experiments will examine corrosion rates under thermal cycling conditions.

ACKNOWLEDGMENT

This work was sponsored by the United States Department of Energy under contract DE-AC04-~~76DP00789~~ 94AL85000.

REFERENCES

1. Hancock, P. *Oxid. Metals* **23,** 305 (1985).
2. Bradshaw, R.W., and Carling, R.W. Sandia National Laboratories, SAND87-8005, April 1987.
3. *Alternate Central Receiver Power Systems, Phase II, Volume III, Molten Salt Materials Tests.* Martin Marietta, MCR-81-1707. May 1981.
4. El Hosary, A.A., Baraka, A., and Abdel-Rohman, A.I. *Brit. Corros. J.*, **11,** 228 (1976).
5. Notoya, T., Ishikawa, T., and Midorikawa, R. Proceedings of the 5th International Congress on Metallic Corrosion, p. 1039 (1972).
6. Kayafa, I. *Corrosion* **36,** 443 (1980).
7. N.A.C.E. Technical Practices Committee, Materials Performance, **6,** 69 (1967).
8. Bradshaw, R.W., Goods, S.H., Prairie, M.R., and Boehme, D.R., *Corrosion of Carbon Steel and Stainless Steels in Molten Nitrate Mixtures.* Proceedings of the International Symposium on Molten Salt Chemistry and Technology - 1993, PV-93-9, p. 446. The Electrochemical Society, May 1993.
9. Nissen, D.A., and Meeker, D.E. *Inorg. Chem.*, **22,** 716 (1982).
10. White, S.H. and Twardoch, U.M. *A Study of the Interactions of Molten Sodium Nitrate-Potassium Nitrate 50 mol% Mixture with Water Vapor and Carbon Dioxide in the Air.* EIC Laboratories, September 1981.

DATE
FILMED
2/4/94
END